JOURNAL OF MATERIALS SCIENCE 13 (1978) 1725–1739

Continuous plastic cracks in ordered alloys

K. JAGANNADHAM, M. J. MARCINKOWSKI
Engineering Materials Group, and Department of Mechanical Engineering, University of Maryland, College Park, Maryland 20742, USA

A discrete dislocation analysis of the continuous plastic crack is carried out for ordered alloys. The crack is assumed to nucleate and reach a size where it will emit a set of lattice dislocations in order to decrease its energy. Further growth of the crack takes place elastically until it can emit the next set of lattice dislocations. Repeated emission of lattice dislocations, with elastic crack growth in between, leads to the Griffith configuration where the energy variation with size of the crack is zero. It is shown that a crack, either tensile or shear, can be stabilized by the presence of antiphase boundary energy alone. In the absence of frictional stress or with the very low frictional stresses encountered in real materials, the lattice dislocations are generated in pairs on each slip plane. However, when the frictional stress is high, the lattice dislocations are generated as single ones, giving rise to an antiphase boundary between the crack and the lattice dislocation.

1. Introduction

In the past, it has been shown that the discrete dislocation analysis of the behaviour of cracks can replace the method of continuous distribution of dislocations and the methods using continuum mechanics, since it satisfies the free surface boundary conditions on the crack surfaces [1, 2] and also because the accuracy of the analysis can be improved by considering larger number of dislocations representing the crack configuration [3]. In addition, the discrete dislocation method has the advantage that it can be used to analyse complex configurations of cracks, namely with respect to their plastic behaviour [1, 4]. It has been found that the behaviour of a crack under an applied stress can be classified in general into four categories, namely elastic, discontinuous plastic, elasto-plastic and continuous plastic [1, 5]. An elastic crack is one where the generation of lattice dislocations in the medium ahead of the crack tip is completely prohibited due to the large frictional stress acting against the movement of the lattice dislocations [5, 6]. The discontinuous plastic crack configuration is obtained when an elastic crack of a given size turns plastic by emitting lattice dislocations so as to reduce its energy [5–7]. When an elastic crack of any size emits a set of lattice dislocations discontinuously and further expands only elastically to reach the Griffith configuration, the configuration obtained is termed an elasto-plastic crack [5]. It has been found that a more realistic crack growth phenomenon would be for a nucleated elastic crack of smallest size to generate a set of lattice dislocations in order to reduce its energy and to expand further elastically until it can emit the next set of lattice dislocations. This is repeated until the crack reaches the Griffith configuration. Repetition of elastic crack growth with intermittent generation of lattice dislocations is found to increase the total energy of the crack configuration above that of all the other categories of crack growth phenomena [1, 4], and is explained by the fresh nucleation of an elastic segment of crack each time, subsequent to generation of lattice dislocations in order to raise the stress field at the tip. The uniqueness of the path followed by the above crack growth process in the energy versus size of crack curve depends, among other factors, on the initial size of the crack. The irreversible frictional work done on the lattice dislocations in moving against the lattice friction induces the crack configuration to

remain stable. It has also been found that a plastic shear crack with the slip plane in the same plane as the crack plane requires much higher energy than that of a plastic tensile crack in order to reach the Griffith configuration, and therefore becomes a very stable configuration. The above crack growth phenomena is termed "continuous plastic crack". In all the above definitions of crack growth phenomena, the crack is assumed to nucleate in a homogeneous medium and expand under the action of a constant applied stress.

In ordered alloys, it is now well established that a dislocation separates into partial dislocations bounded by an antiphase boundary. Such a dislocation is termed a superlattice dislocation, and is characterized by the property that it reproduces the correct periodicity of the crystal as it glides through the lattice. In the absence of an applied stress, the equilibrium configuration of the superlattice dislocation is obtained by balancing the repulsive force between the partial dislocations by the attractive force produced by the antiphase boundary energy. It is useful and interesting to consider the formation of the continuous plastic crack in an ordered alloy since the formation of the superlattice dislocations is expected to lead to interesting features in the crack growth and the dislocation configuration of the crack. In order to simplify the analysis, the simplest type of ordered alloy, namely the CsCl or B2 type, is considered. Still more specifically, only one particular B2 type alloy will be considered in any great detail; namely Fe–Co. This choice was made since Fe–Co can be studied in both the ordered and disordered states and the degree of ordering can be varied. The antiphase boundary energy can be varied either by heat treatment and/or by changing the atomic percentage of the solute atoms [8]. It is assumed that the superlattice dislocation consists of two $a/2\ \langle 1\,1\,1\rangle$ type partials bounded by an antiphase boundary. This structure of the superlattice dislocation will also be applicable to superlattice dislocations in Fe–Al alloys. The formation of other types of superlattice dislocations is not considered here although the method can also be extended in principle to such configurations.

It has been found that atomic ordering leads to intercrystalline crack formation in FeCo [9], but to transgranular cleavage in FeCo–2V [10]. The present analysis of crack growth by continuous generation of lattice dislocations with the expansion of the crack will be applicable to both types of crack formation observed in ordered alloys. The emphasis here is with respect to the configuration of the crack formed with lattice dislocations generating the antiphase boundary around the crack. It is seen from Fig. 1 that when the elastic crack in an ordered alloy turns plastic, generating lattice dislocations, the structure of the lattice dislocation on the slip plane consists of either a dislocation of Burgers vector $a/2\ \langle 1\,1\,1\rangle$ connected to the crack by an antiphase boundary, e.g. Fig. 1a or else two dislocations each of Burgers vector $a/2\ \langle 1\,1\,1\rangle$ connected by an antiphase boundary, but not separated from the crack by an antiphase boundary, e.g. Fig. 1b. Since the lattice dislocations move in the presence of a frictional stress opposing their movement, the antiphase boundary energy created adds to the frictional energy when the lattice dislocations are created. Therefore, it is interesting to investigate the effect of the addition-

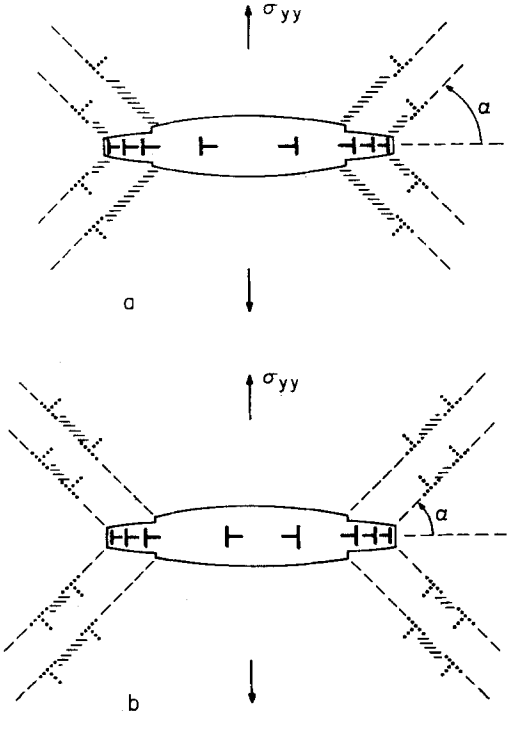

Figure 1 (a) Schematic illustration of the formation of the plastic zone at the tip of a tensile crack. The plastic zone consists of lattice dislocations generated on the slip plane and connected to the crack region by an antiphase boundary. The hatched region is the antiphase boundary. (b) Same as Fig. 1a except that the plastic zone consists of lattice dislocations generated in pairs on the slip plane and bound by an antiphase boundary. The pairs are separated from the crack region. The hatched region is the antiphase boundary.

al antiphase boundary energy created on continuous plastic crack formation. While the frictional energy expended in moving the lattice dislocations is irreversible, the antiphase boundary energy created is reversible.

2. Analysis of continuous plastic tensile cracks in ordered alloys

An elastic crack of the smallest size that can emit lattice dislocations in order to decrease its energy is considered. After the first set of lattice dislocations is generated, the crack size is incremented to a level where it can emit the next set of lattice dislocations. This procedure is repeated until the total energy of the crack configuration does not increase further with increase in size of the crack. The configuration obtained at this point is considered as the Griffith configuration of the continuous plastic tensile crack. The total energy of the crack with its plastic zone is given by

$$E_T = E_S + E_I + E_\tau + E_\gamma + E_f + E_P + E_L$$

where E_S is the total self energy of the crack dislocations and lattice dislocations, E_I the interaction energy between all the dislocations, E_τ the work done by the applied stress on the crack dislocation and lattice dislocations, E_γ the surface energy created, E_f the frictional work done in the movement of the lattice dislocations against the frictional stress, E_P the antiphase boundary energy created in generating the lattice dislocations and E_L the additional surface energy due to the formation of ledges at the crack tip whenever a lattice dislocation is emitted. The expressions for the self energies and interaction energies of dislocations are obtained from the standard formulae [11]. It should be pointed out that the frictional energy expended at any point in the crack growth will be that required in the movement of lattice dislocations at that particular stage plus the frictional energy expended previous to this increment of crack growth. Thus, the frictional energy is cumulative. In order to determine the positions of the dislocations, the total energy of the configuration is minimized with respect to the positions of all the dislocations. In particular,

$$E_{T_D} = E_S + E_I + E_\tau + E_f + E_P + E_L \qquad (2)$$

is minimized using the minimization subroutine entitled Funfit [12]. Each time the crack is filled with as many crack dislocations as it can accommodate so that the free surface boundary condition is satisfied on the crack surface. The Burgers vector of the lattice dislocations in an ordered alloy is taken as $\mathbf{b}_L = a/2\langle 111\rangle$ where a is the lattice parameter. The Burgers vector of the crack dislocations is given by $\mathbf{b}_c = 2\mathbf{b}_L \sin\alpha$ where α is the angle between the slip plane and the crack plane. This relationship is obtained from the conservation of Burgers vectors. The values assumed for the elastic constants μ and ν and the surface energy γ are $\mu = 7.14 \times 10^{11}$ dynes cm^{-2}, $\nu = 0.3333$ and $\gamma = 1950$ ergs cm^{-2}. The antiphase boundary energy γ_P was varied from zero to 120 ergs cm^{-2} in order to consider the variation in degree of order. In a completely disordered alloy, $\gamma_P = 0$, while $\gamma_P = 120$ in a completely ordered alloy.

2.1. Results and discussion

In the present analysis, the applied stress level is assumed at relatively high values so that the Griffith crack configuration of the plastic crack is achieved at smaller sizes of crack, thereby reducing the computer time required to reach this configuration. The component of applied stress on the slip plane becomes high except when the slip plane is inclined to crack plane at 90° or closer to 90°. When a high frictional stress level is maintained to stabilize the crack, the contribution from the frictional energy becomes sufficiently large so as to mask the effect of the antiphase boundary energy. In reality, the applied stress level is much

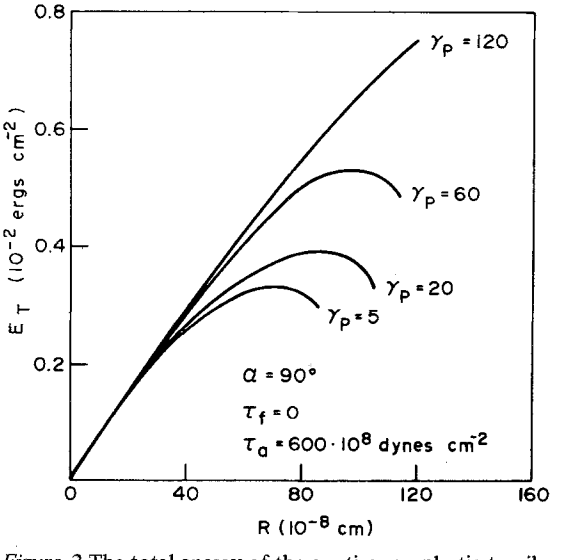

Figure 2 The total energy of the continuous plastic tensile crack, E_T shown against the size of the crack R for various values of γ_P. Note the frictional stress is zero.

smaller and the crack size is much bigger. The frictional stress level on the slip plane required to stabilize the crack is also much smaller so that the frictional energy cannot be very large and the realistic behaviour of the plastic crack depends strongly on the antiphase boundary energy. In order to distinctly show this difference in the behaviour of the cracks, the calculations were performed with zero friction and the slip plane inclined normal to the crack plane. Although the applied stress level is large, the component of the applied stress on the slip plane inclined at 90° is zero and hence the realistic behaviour of the crack can be understood from this idealized case.

The total energy versus crack size curves for a continuous plastic tensile crack are shown in Fig. 2 for $\alpha = 90$ degrees, and applied stress $\tau_a = 600 \times 10^8$ dynes cm^{-2} and a frictional stress $\tau_f = 0$. It was seen that in the absence of frictional stress, the lattice dislocations generated on the slip plane do not move away indefinitely from the crack as they would in a fully disordered alloy. On the contrary, the lattice dislocations were observed to come out in pair bounded by antiphase boundary and occupy equilibrium positions from the crack region. This stabilizing action of the antiphase boundary energy in the absence of frictional stress is achieved due to the fact that when the pair of lattice dislocations generated moves along the slip plane under the action of the gradient of crack tip stress field, the distance between the two lattice dislocations in the pair increases, thereby increasing the antiphase boundary energy contribution to the total energy of the crack. This increase in energy of the superlattice dislocations with distance creates an opposing force on them which keeps them from moving away from the crack tip indefinitely. The dislocation configuration of the continuous plastic crack is shown schematically in Fig. 3a. Since the crack size was much smaller compared to the distance to which lattice dislocations had moved, only a schematic sketch is given in Fig. 3a showing the distance of separation of the lattice dislocations bounded by antiphase boundary. The equilibrium separation between the partials in the superlattice dislocation

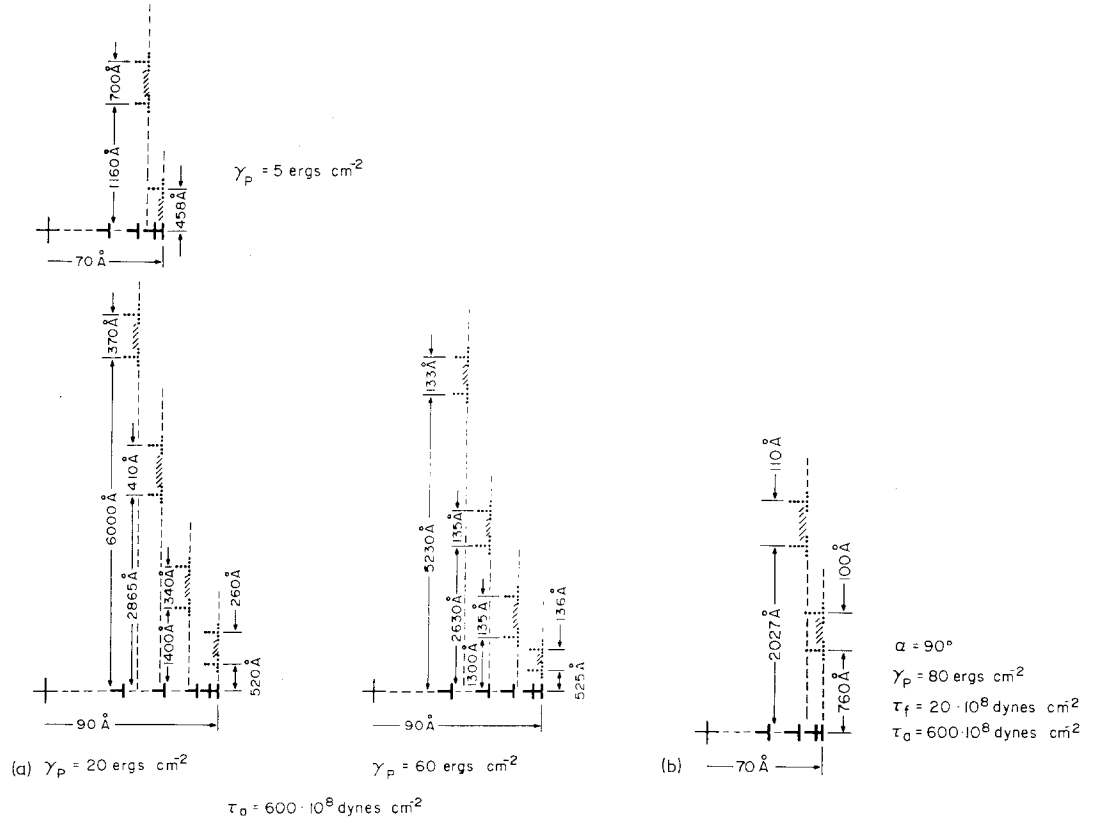

Figure 3 (a) Schematic illustration of the dislocation configuration of the continuous plastic Griffith crack at various values of γ_P for $\tau_f = 0$ $\tau_a = 600 \times 10^8$ dynes cm^{-2}. The figures are not drawn to scale. Also, only one quadrant of the symmetric crack configuration is shown. The hatched region corresponds to the antiphase boundary. (b) Same as Fig. 3a but with $\gamma_P = 80$ and $\tau_f = 20 \times 10^8$ dynes cm^{-2}.

at $\gamma_P = 5\,\text{ergs cm}^{-2}$ in the absence of the crack stress field is 2000 Å, at $\gamma_P = 20\,\text{ergs cm}^{-2}$, it becomes 500 Å and at $\gamma_P = 60\,\text{ergs cm}^{-2}$ it becomes 170 Å. It is seen that the separation between the partials at all three values of γ_P around the crack remains less than the equilibrium distance of separation between the partials in the absence of the crack stress field. This may be explained by the fact that the stress due to the crack acting on leading partials is less than the stress acting on the trailing partial. It is seen from the E_T versus R curves in Fig. 2, that the total energy of the crack increases and the size of the Griffith crack corresponding to the maximum in E_T versus R is also higher as γ_P increases. The maximum in E_T versus R for $\gamma_P = 120\,\text{ergs cm}^{-2}$ could not be obtained due to the excessive computer time required. Table I shows the breakdown of energy contributions associated with a continuous plastic tensile crack for three values of γ_P. The crack reaches the Griffith configuration at a smaller value of R_c for smaller value of γ_P. Therefore the crack is emitting more lattice dislocations with increasing γ_P, leading to larger values of the self energy of crack dislocations E_{S_C} and lattice dislocation, E_{S_L}. The interaction energy of the crack dislocations, E_{I_C} and lattice dislocations E_{I_L} and the work done by the applied stress in creating the crack configuraration, E_T which is negative, increase. Thus, the total energy of the crack configuration increases. It should be pointed out that since the energy due to antiphase boundary formation is a reversible term, and because $\tau_f = 0$, the configuration obtained is reversible and one can move on the E_T versus R curves in either direction. Therefore, when the applied stress is removed, the crack collapses completely leaving no dislocation configuration. It is clear from the results obtained from the continuous plastic tensile crack that when the frictional stress is very small, the lattice dislocations are generated in pairs on the slip plane and the configuration corresponds to the one shown in Fig. 1b.

TABLE I Breakdown of energy contributions associated with a continuous plastic tensile crack in an ordered alloy. The applied stress $\tau_a = 600 \times 10^8$ dynes cm^{-2} and $\tau_f = 0$. The slip plane is normal to the crack plane

γ_P	(ergs cm^{-2})	5	20	60
R_C	(10^{-8} cm)	70	90	90
N_C		4	5	5
N_L		3	8	8
E_γ	(10^{-3} ergs cm^{-1})	5.460	7.020	7.020
$E_{\gamma P}$	(10^{-3} ergs cm^{-1})	0.244	1.152	1.283
E_{S_C}	(10^{-3} ergs cm^{-1})	5.973	7.466	7.466
E_{S_L}	(10^{-3} ergs cm^{-1})	8.959	23.980	23.890
E_{I_C}	(10^{-3} erts cm^{-1})	− 2.078	− 1.721	− 1.700
E_{I_L}	(10^{-3} ergs cm^{-1})	− 5.228	−11.100	−10.100
$E_{I_{CL}}$	(10^{-3} ergs cm^{-1})	0.247	0.656	0.717
E_T	(10^{-3} ergs cm^{-1})	−10.769	−24.712	−24.681
E_L	(10^{-3} ergs cm^{-1})	0.500	1.360	1.360
E_T	(10^{-3} ergs cm^{-1})	3.300	3.900	5.280

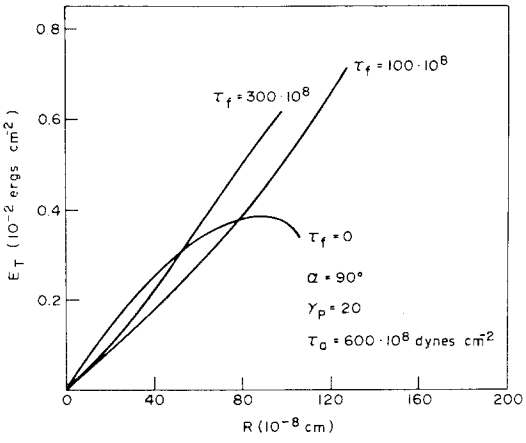

Figure 4 E_T versus R curve for three values of frictional stress, τ_f, $\alpha = 90°$, $\gamma_P = 20$ ergs cm $^{-2}$.

When the slip plane is not normal to the crack plane, i.e. $\alpha \neq 90°$, the applied stress has a component of shear stress acting on the slip plane which aids the movement of the lattice dislocations away from the crack tip. When the applied stress level is small and the crack size is large, the results obtained earlier are once again applicable since only very small frictional stress is necessary to stabilize the crack. It is expected that this observed behaviour is realistic in most materials. It is seen from Fig. 4 that the continuous plastic tensile crack requires very high energy to reach the Griffith configuration when high frictional stress is included on the slip plane at $\alpha = 90°$. The behaviour of the crack for low frictional stresses is similar to that obtained with zero friction. As an example of the dislocation configuration obtained at the Griffith stage when low frictional stress is applied, Fig. 3b shows the continuous plastic tensile crack for $\alpha = 90°$ and $\gamma_P = 80\,\text{ergs cm}^{-2}$. It is seen that the lattice dislocations are given out in pairs bounded by antiphase boundary. Since the antiphase boundary energy is very large, the separation between the lattice dislocations in the pair is small and found to be 100 Å, but its value is still smaller than the equilibrium value in

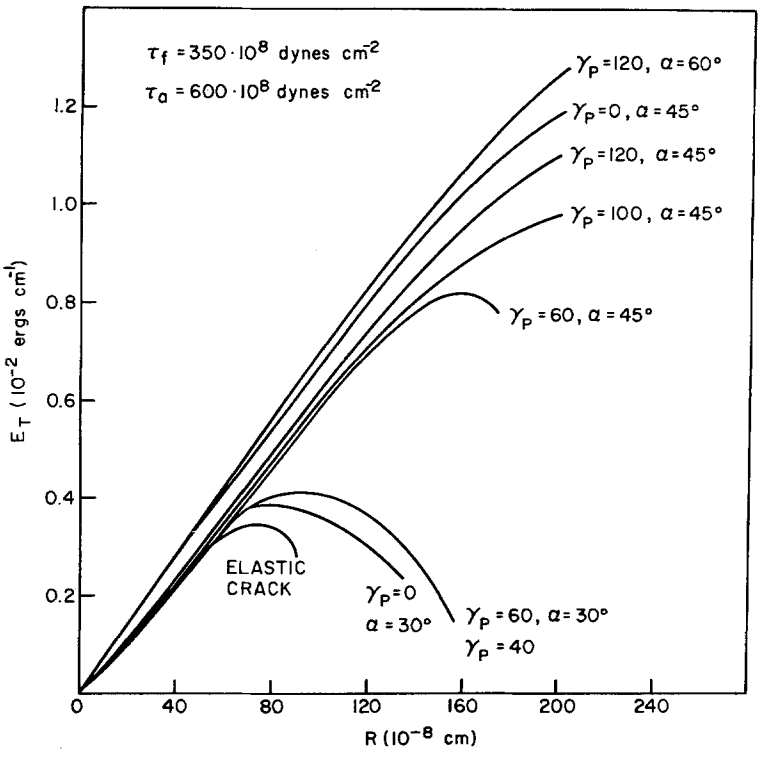

Figure 5 E_T versus R curve shown for different values of α and γ_P. The curve for an elastic crack is also shown. $\tau_f = 350 \times 10^8$ dynes cm^{-2}.

the absence of frictional stress and the crack. When the applied stress level is large and the slip plane is inclined to the crack plane at values of α much smaller than $\alpha = 90°$, the frictional stress required to stabilize the crack will also be higher. The shear stress component of the applied stress reaches a maximum when $\alpha = 45°$. However, the crack tip stress field is relaxed to the maximum when the lattice dislocations are generated on slip planes at $\alpha = 90°$. These two stress fields have their maximum effect for $\alpha = 60°$. It is seen from Fig. 5 that for $\gamma_P = 120$, the Griffith configuration is not reached for $\alpha = 60°$ and the curve remains above those for $\alpha = 45°$. For $\alpha = 45°$, the maximum in the E_T versus R is obtained only for $\gamma_P = 60$. When $\gamma_P < 60$, the lattice dislocations move very large distances giving rise to more frictional energy and antiphase boundary energy and therefore the crack behaves like a high energy crack. On the other hand, for $\gamma_P > 60$, the contribution from the antiphase boundary energy becomes greater, once again making the crack require very high energy to reach the Griffith configuration. Thus, for a given level of frictional stress, there is a range of values of γ_P for which the maximum in the E_T versus R curve could be obtained and all other configurations correspond to high energy cracks. When $\alpha = 30°$, the shear stress component of the applied stress on the slip plane becomes smaller and also, the crack cannot relax its energy to the same content on the slip plane. Since these two factors are not favourable, the crack tends to become less plastic. Therefore, the lattice dislocations cannot move larger distances. The E_T versus R curves are shown in Fig. 5 for $\gamma_P = 0$, 40 and 60 for $\alpha = 30°$. Above $\gamma_P = 60$, the crack behaves completely elastically before it reaches the Griffith configuration. Thus, increasing the antiphase boundary tends to make the crack elastic. The dislocation configurations obtained at $\tau_f = 350 \times 10^8$ dynes cm^{-2} and $\alpha = 30°$ and 45° are shown in Fig. 6. In contrast to the configuration obtained for $\alpha = 90°$ and $\tau_f = 0$ where the lattice dislocations are generated in pairs on each slip plane, the configurations shown in Fig. 6 have a single dislocation on each slip plane, connected by an antiphase boundary to the crack. Here the frictional energy becomes larger if a pair of lattice dislocations is generated, thus only one lattice dislocation is generated each time on the slip plane. This configuration corresponds to that shown in Fig. 1a. It is also seen that for $\alpha = 30°$, the crack generates only one lattice dislocation, thus be-

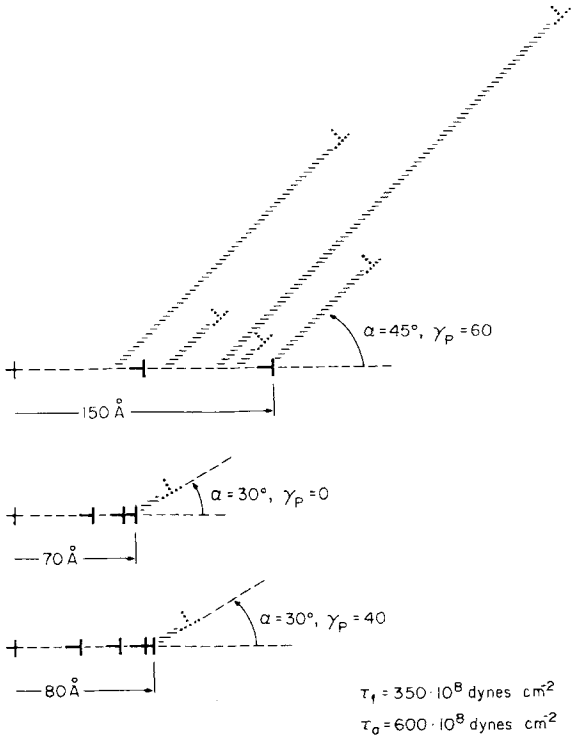

Figure 6 Dislocation configuration of a continuous plastic tensile crack in an ordered alloy for two values of α. The hatched region is the antiphase boundary. Only one quadrant of the crack configuration is shown since it is symmetrical with respect to x and y.

coming less plastic with decreasing α and increasing γ_P. Tables II and III show the breakdown of energy contributions associated with the tensile crack at $\alpha = 45°$ and 30°. At $\tau_f = 350 \times 10^8$ dynes cm^{-2}, the crack size and the total energy of the crack for $\alpha = 45°$ are approximately twice that for $\alpha = 30°$. The number of lattice dislocations generated for $\alpha = 45°$ is high and therefore the antiphase boundary energy is also greater. Associated with the larger number of lattice dislocations, the frictional energy and the work done by the applied stress are also large for $\alpha = 45°$, leading to a higher value of the total energy of the crack. It is seen from Table III that for $\alpha = 30°$, the Griffith crack configuration increases its size by a small value only because the crack tends to be less plastic and the contribution from the antiphase boundary is very small. Therefore, the total energy of the crack also does not increase very much. The E_T versus R curves are shown in Fig. 7 for various values of α when $\tau_f = 300 \times 10^8$ dynes cm^{-2}. When $\alpha = 60°$, the E_T versus R curve could not be shown since the crack moves the lattice dislocations to very large distances due to the large value of shear stress on the slip plane compared to frictional stress. The shear stress component of applied stress reaches a maximum of 300×10^8 dynes cm^{-2} for $\alpha = 45°$ which is also equal to the frictional stress. Therefore, in the absence of antiphase boundary energy, the crack configuration is unstable. Fig. 7 shows the E_T versus R curve for $\alpha = 45°$ and for various values of γ_P. When $\gamma_P <$ 60 ergs cm^{-2}, the crack requires higher energy to reach the Griffith configuration and hence these could not be obtained. The total energy of the crack E_T and the size of the crack R_C decrease with increasing γ_P. The dislocation configurations obtained at $\tau_f = 300 \times 10^8$ dynes cm^{-2} are shown in Fig. 8a for two values of α. It is seen that the

TABLE II Breakdown of energy contributions associated with a continuous plastic tensile crack in an ordered alloy. The applied stress $\tau_a = 600 \times 10^8$ dynes cm^{-2} and the frictional stress τ_f takes two values. The slip plane is inclined to the crack plane by 45°

τ_f	(10^{-8} dynes cm^{-2})	300	300	300	350
γ_P	(ergs cm^{-2})	80	100	120	60
R_C	(10^{-8} cm)	170	110	70	150
N_C		3	2	2	2
N_L		6	4	2	5
E_γ	(10^{-3} ergs cm^{-1})	13.260	8.580	5.460	11.700
$E_{\gamma P}$	(10^{-3} ergs cm^{-1})	5.629	2.290	0.938	14.600
E_{S_C}	(10^{-3} ergs cm^{-1})	8.801	5.867	5.867	5.867
E_{S_L}	(10^{-3} ergs cm^{-1})	17.920	11.950	5.973	14.930
E_{I_C}	(10^{-3} ergs cm^{-1})	−3.228	−3.486	−3.442	−3.443
E_{I_L}	(10^{-3} ergs cm^{-1})	−2.430	−3.960	−3.090	−2.750
$E_{I_{CL}}$	(10^{-3} ergs cm^{-1})	8.669	3.800	1.735	5.085
E_f	(10^{-3} ergs cm^{-1})	45.280	14.730	5.030	18.280
E_τ	(10^{-3} ergs cm^{-1})	−85.740	−33.310	−14.070	−43.870
E_L	(10^{-3} ergs cm^{-1})	1.020	0.608	0.334	0.835
E_T	(10^{-3} ergs cm^{-1})	9.161	7.124	4.733	8.101

TABLE III Breakdown of energy contributions associated with a continuous plastic tensile crack in an ordered alloy. The applied stress $\tau_a = 600 \times 10^8$ dynes cm^{-2}. The frictional stress τ_f takes three values. The slip plane is inclined to the crack plane by 30°

τ_f	(10^8 dynes cm^{-2})	350	350	350	300	300	300	250	250	250
γ_P	(ergs cm^{-2})	0	40	60	80	100	120	40	80	120
R_C	(10^{-8} cm)	70	80	80	70	70	70	80	60	70
N_C		3	4	4	3	3	3	4	3	4
N_L		1	1	1	1	1	1	2	1	1
E_γ	(10^{-3} ergs cm^{-1})	5.460	6.240	6.240	5.460	5.460	5.460	6.240	4.680	5.460
$E_{\gamma P}$	(10^{-3} ergs cm^{-1})	0	0.041	0.053	0.100	0.105	0.106	0.934	0.270	0.338
E_{S_C}	(10^{-3} ergs cm^{-1})	4.483	5.977	5.977	4.483	4.483	4.483	5.977	4.483	5.977
E_{S_L}	(10^{-3} ergs cm^{-1})	2.986	2.986	2.986	2.986	2.986	2.986	5.973	2.986	2.986
E_{I_C}	(10^{-3} ergs cm^{-1})	−2.010	−2.186	−2.212	−1.983	−2.003	−2.022	−2.022	−2.054	−2.391
E_{I_L}	(10^{-3} ergs cm^{-1})	−2.048	−2.035	1.305	−2.026	−2.042	−2.058	−3.306	−1.932	−1.946
$E_{I_{CL}}$	(10^{-3} ergs cm^{-1})	0.995	1.264	1.305	0.936	0.980	1.022	1.014	0.564	0.813
E_f	(10^{-3} ergs cm^{-1})	0.743	0.770	0.657	0.808	0.679	0.568	1.252	1.807	1.508
E_τ	(10^{-3} ergs cm^{-1})	−6.921	−9.167	−9.050	−7.104	6.966	−6.843	−23.361	−7.328	−8.904
E_L	(10^{-3} ergs cm^{-1})	0.167	0.167	0.167	0.167	0.167	0.167	0.334	0.167	0.167
E_T	(10^{-3} ergs cm^{-1})	3.857	4.056	4.075	3.826	3.849	3.869	4.305	3.642	4.007

number of lattice dislocations generated decreases with increasing γ_P because the Griffith size is smaller. It is seen from the energy contributions given in Table II for $\tau_f = 300 \times 10^8$ dynes cm^{-2} that the self energy of crack dislocations and lattice dislocations, the frictional energy, the antiphase boundary energy and the work done by the applied stress increase, leading to an increase in the total energy of the crack, E_T with decreasing γ_P. A direct comparison between energy contributions to the total energy at two values of τ_f given in Table II is not possible due to different value of γ_P. At $\alpha = 30°$, the crack tip stress field is not very large although the component of the applied stress has the same value as that for $\alpha = 60°$. Therefore, the Griffith crack configuration is achieved with $\tau_f = 300 \times 10^8$ dynes cm^{-2} and the presence of antiphase boundary energy, although the same is not true for $\alpha = 60°$ for reasons mentioned earlier. It is seen from Fig. 7 that the change in E_T with increasing γ_P is very small at $\alpha = 30°$ since only one lattice dislocation is generated. Fig. 8a shows that increasing γ_P makes the lattice dislocation move smaller distances on the slip plane. When the frictional stress is further reduced to 250×10^8 dynes cm^{-2} for $\alpha = 30°$, the crack becomes un-

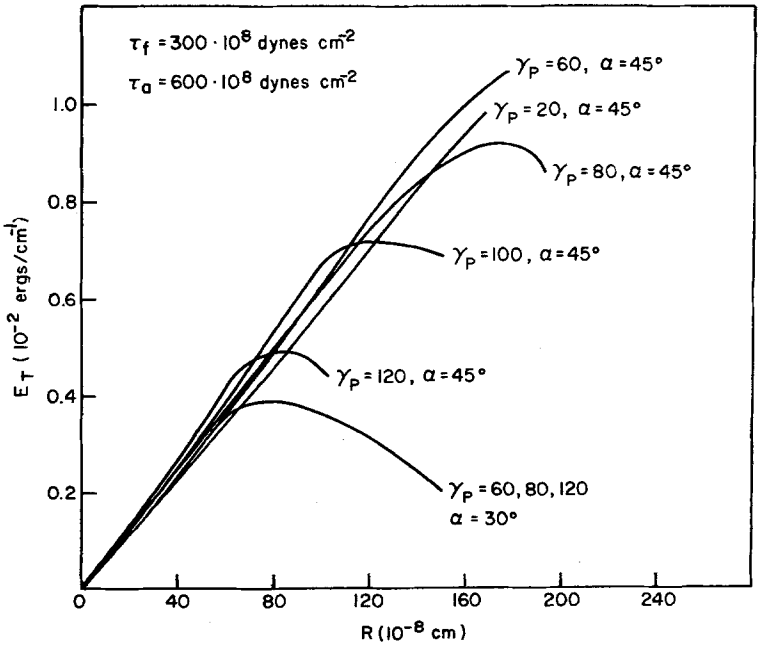

Figure 7 E_T versus R curve shown for different values of α and γ_P, $\tau_f = 300 \times 10^8$ dynes cm^{-2}.

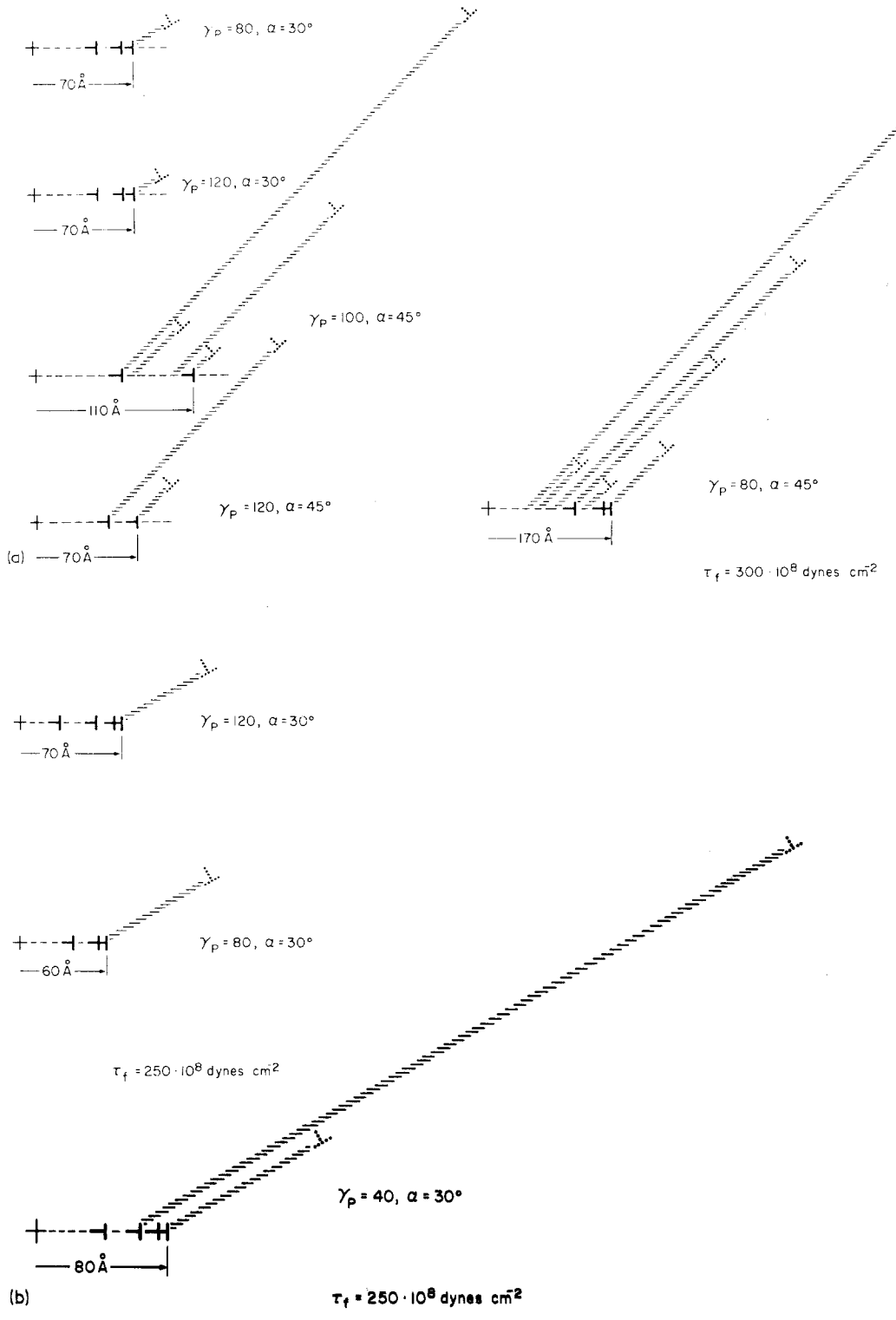

Figure 8 (a) Dislocation configuration of a continuous plastic crack in an ordered alloy for $\tau_f = 300 \times 10^8$ dynes cm^{-2} and two values of α. (b) Same as Fig. 8a but $\tau_f = 250 \times 10^8$ dynes cm^{-2}.

stable for $\gamma_P < 40\,\text{ergs cm}^{-2}$. As seen in Fig. 8b, increasing γ_P decreases the distance by which the lattice dislocations move on the slip plane. It is seen from Table III that the maximum energy configuration is reached at a larger size for $\gamma_P =$ 40 or $120\,\text{ergs cm}^{-2}$, but at a smaller size for $\gamma_P = 80$. When $\gamma_P = 40$, the lattice dislocations move large distances, contributing a higher value of antiphase boundary energy. When $\gamma_P = 120$, the lattice dislocations move shorter distances, but due to the high value of γ_P, the antiphase boundary energy contribution is still high. At $\gamma_P = 80$, the lattice dislocations cannot move larger distances and therefore the total energy is smaller.

It becomes clear from the present study that there are two types of configurations of the continuous plastic tensile crack observed in ordered alloys. When the frictional stress is small, the configuration obtained will be that of the crack surrounded by pairs of lattice dislocations connected by an antiphase boundary. When the frictional stress is high, the configuration obtained will be that of crack surrounded by single lattice dislocations connected to the crack by an antiphase boundary. The frictional stress values in materials is very small and hence the configuration given in Fig. 1b is more favourable.

3. Analysis of continuous plastic shear cracks in ordered alloys

The discrete dislocation analysis of the continuous plastic shear crack is carried out along the same lines as that of a continuous plastic tensile crack. The shear crack is represented by edge dislocations whose Burgers vector is parallel to the free surface of the crack. The computational procedure followed is similar to that of a tensile crack. The lattice dislocations have the Burgers vector equal to $a/2\langle 111\rangle$ where a is equal to the lattice parameter. The Burgers vector of the crack dislocations is determined from the conservation of Burgers vectors which gives $\mathbf{b_C} = 2\mathbf{b_L}\cos\alpha$ All other parameters used have the same value as those for a plastic tensile crack. It is important to note that the applied stress has a component on the slip plane which reaches its maximum on a slip plane for which $\alpha = 0$ and decreases with increasing α. The relaxation of the crack tip stress field is also a maximum when $\alpha = 0$. Therefore, the crack tends to be more plastic for $\alpha = 0$ and becomes a very high energy configuration [1]. The tendency for plastic zone formation decreases with increasing α since both the component of applied stress and the crack tip stress field decrease. At $\alpha = 90°$, the crack behaves completely elastically.

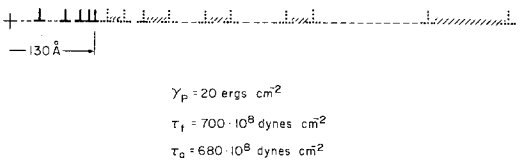

Figure 9 Dislocation configuration of a continuous plastic shear crack in an ordered alloy when $\alpha = 0$. Only one half of the configuration is shown since it is symmetric about the y-axis. Note the way in which the lattice dislocations are arranged in pairs bounded by antiphase boundary.

3.1. Results and discussion

Fig. 9 shows the dislocation configuration of a plastic shear crack before it reached the Griffith configuration since the Griffith configuration could not be reached due to excessive computer time required. It is seen that the lattice dislocations are always generated in pairs in order to reduce the antiphase boundary energy. The distance between the partials of the superlattice dislocation decreases as the crack tip is approached and the distance of separation between the pairs is larger than the width of the antiphase boundary connecting the pair. It has not been possible to show all the lattice dislocations in the configuration of Fig. 9 since some of them are situated very far away from the crack tip. It is once again seen that the distance of separation between the partials is less than the equilibrium distance of separation. This may be explained by the unequal crack tip stress field acting on the lattice dislocations on the slip plane.

It is concluded from the previous analysis [1] as well as the present one, that the presence of the antiphase boundary energy in the behaviour of a continuous plastic shear crack in an ordered alloy, when $\alpha = 0$, requires high energy to reach the Griffith crack configuration. The high energy of the configuration for $\alpha = 0$ is explained by the fact that the crack tip can move forward only by moving the lattice dislocation ahead of it and this movement against frictional stress requires very high energy for the crack to reach the Griffith configuration. When the slip plane is at an angle to the crack plane, i.e. $\alpha \neq 0$, the crack tip can move forward without necessarily moving the lattice

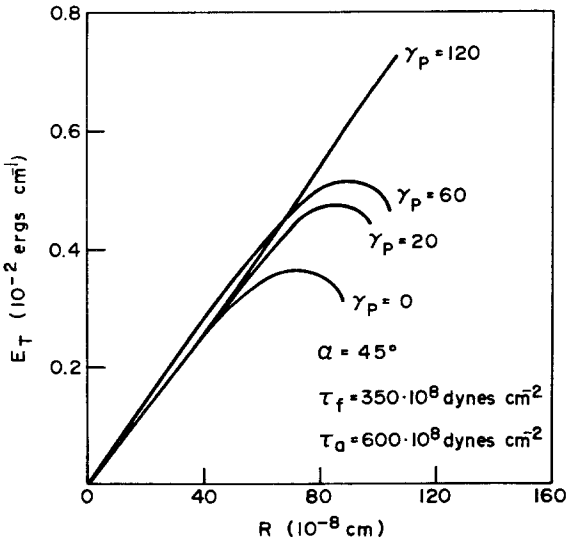

Figure 10 E_T versus R shown for a continuous plastic shear crack in an ordered alloy shown for different values of γ_P. $\alpha = 45°$ and $\tau_f = 350 \times 10^8$ dynes cm^{-2}.

dislocation ahead of it, and therefore there is not a considerable increase in frictional energy. Fig. 10 shows the E_T versus R curves for $\alpha = 45°$, $\tau_f = 350 \times 10^8$ dynes cm^{-2} and various values of γ_P. It is seen that with increasing γ_P, the crack takes more energy to reach the Griffith configuration. The size of the crack at the Griffith configuration also increases with increasing γ_P. When γ_P is 120 ergs cm^{-2}, the maximum on the E_T versus R curve could not be obtained due to the excessive computer time required. The dislocation configuration obtained at $\tau_f = 350 \times 10^8$ dynes cm^{-2} and $\alpha = 45°$ is shown in Fig. 11 for the three values of γ_P. It is seen that initially lattice dislocations are generated in pairs, but in the latter stages of crack growth only single lattice dislocations are generated. In the initial stage, when the crack is completely elastic, there could be sufficient stress relaxation by the generation of a pair of lattice dislocations so as to reduce the antiphase boundary energy, whereas in the latter stages, the stress field of the crack tip is not sufficient to accomplish this. Since the crack size is bigger at $\gamma_P = 60$ ergs cm^{-2} the lattice dislocations have also moved larger distances than when the antiphase boundary energy is zero. Thus, the crack tends to be more plastic. The energy contributions that make up to the total energy of the crack for $\alpha = 45°$ are shown in Table IV. It is seen that the antiphase boundary energy increases with increasing γ_P due to the increase in the number of lattice dislo-

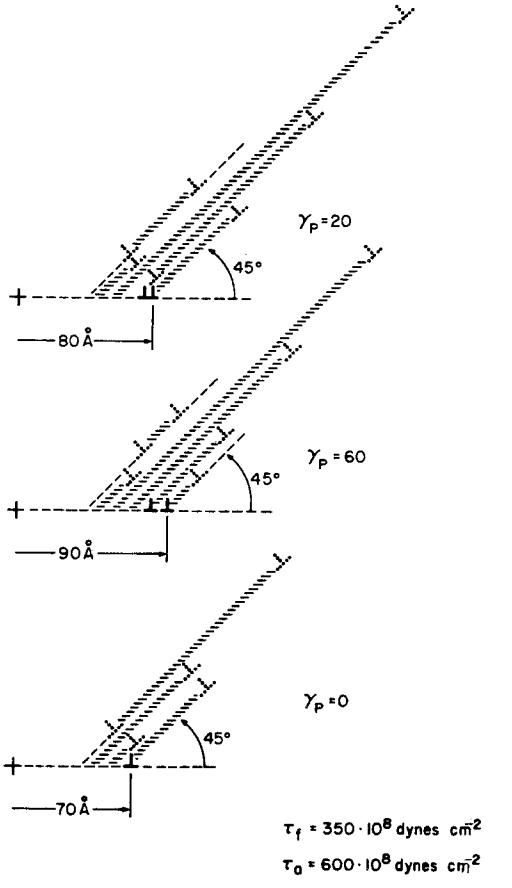

Figure 11 Dislocation configuration of a continuous plastic shear crack in an ordered alloy with the slip plane inclined at 45° to the crack plane. Only one quadrant of the configuration is shown since it is symmetrical about the x-and y-axes. The hatched region is the antiphase boundary.

TABLE IV Breakdown of energy contributions associated with a continuous plastic shear crack in an ordered alloy. The applied stress $\tau_a = 600 \times 10^8$ dynes cm^{-2} and the frictional stress $\tau_f = 350 \times 10^8$ dynes cm^{-2}. The slip plane is inclined to the crack plane by 45°

γ_P	(ergs cm^{-2})	0	20	60
R_C	(10^{-8} cm)	70	80	90
N_C		1	2	2
N_L		5	7	7
E_γ	(10^{-3} ergs cm^{-1})	55.460	6.240	7.020
$E_{\gamma P}$	(10^{-3} ergs cm^{-1})	0	0.425	1.182
E_{S_C}	(10^{-3} ergs cm^{-1})	2.930	5.860	5.860
E_{S_L}	(10^{-3} ergs cm^{-1})	14.930	20.900	20.900
E_{I_C}	(10^{-3} ergs cm^{-1})	− 2.112	− 3.162	− 3.266
E_{I_L}	(10^{-3} ergs cm^{-1})	− 9.600	−11.795	−11.350
$E_{I_{CL}}$	(10^{-3} ergs cm^{-1})	1.142	2.924	2.896
E_f	(10^{-3} ergs cm^{-1})	10.900	19.110	17.850
E_τ	(10^{-3} ergs cm^{-1})	−21.337	−36.914	−37.135
E_L	(10^{-3} ergs cm^{-1})	0.835	1.169	1.169
E_T	(10^{-3} ergs cm^{-1})	3.642	4.758	5.135

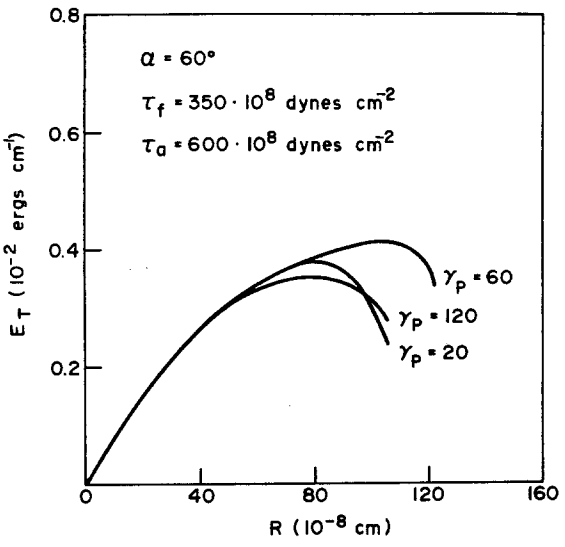

Figure 12 E_T versus R shown for a continuous plastic shear crack in an ordered alloy illustrated for different value of γ_P, $\alpha = 60°$ and $\tau_f = 350 \times 10^8$ dynes cm^{-2}.

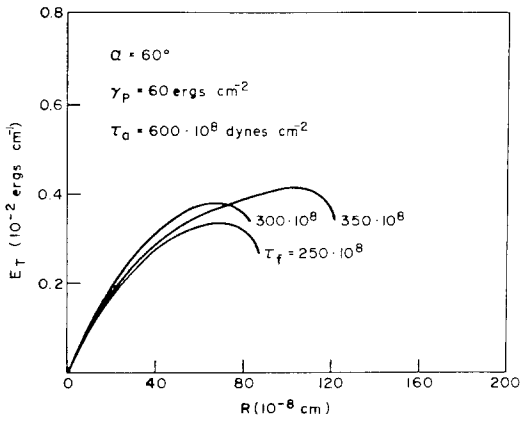

Figure 13 E_T versus R shown for three values of frictional stress for a continuous plastic shear crack in an ordered alloy, $\gamma_P = 60$ ergs cm^{-2} and $\alpha = 60°$.

cations. Since the lattice dislocations have moved shorter distances when $\gamma_P = 60$ than when $\gamma_P = 20$, the frictional energy expended is also smaller, but it is much larger compared to the configuration when $\gamma_P = 0$. When the slip plane is inclined at 60° to the crack plane, the shear stress component of applied stress becomes smaller compared to the value when $\alpha = 45°$. The relaxation of the crack tip stress field is also smaller when $\alpha = 60°$. Therefore, the crack tends to be less plastic. The total energy versus crack size curves for $\alpha = 60°$ are shown in Fig. 12 for three values of γ_P. The dislocation configurations obtained at the Griffith stage are shown in Fig. 14. The Griffith size of the crack increases initially with increasing γ_P but the crack tends to become less plastic when γ_P is large. The energy contributions associated with the plastic shear crack for $\alpha = 60°$ are shown in Table V.

It is seen that for $\gamma_P = 60$ ergs cm^{-2} the crack size is large and it emits a large number of lattice dislocations, thereby increasing the total energy, but either below that value of γ_P or above it, the crack reaches the Griffith configuration at a smaller value and therefore the total energy is also small. The crack generates only one dislocation at a time. The total energy versus size curves for $\gamma_P = 60$ ergs cm^{-2} and different values of frictional stress are shown in Fig. 13. It is seen that with decreasing friction, the crack tends to reach the Griffith configuration at a smaller value. However, further decrease of τ_f, makes the crack

TABLE V Breakdown of energy contributions associated with a continuous plastic shear crack in an ordered alloy. The applied stress $\tau_a = 600 \times 10^8$ dynes cm^{-2}. The slip plane is inclined to the crack plane by 60°

τ_f	(10^8 dynes cm^{-2})	350	350	350	350	300	250
γ_P	(ergs cm^{-2})	0	20	60	120	60	60
R_C	(10^{-8} cm)	70	80	110	80	60	70
N_C		2	3	5	4	3	2
N_L		3	3	6	1	2	3
E_γ	(10^{-3} ergs cm^{-1})	5.460	6.240	8.580	6.240	4.680	5.460
$E_{\gamma P}$	(10^{-3} ergs cm^{-1})	0	0.047	0.401	0.087	0.104	0.130
E_{SC}	(10^{-3} ergs cm^{-1})	2.982	4.473	7.455	5.964	4.473	2.982
E_{SL}	(10^{-3} ergs cm^{-1})	8.959	8.959	17.920	2.986	5.973	8.959
E_{IC}	(10^{-3} ergs cm^{-1})	−1.551	1.914	− 0.046	−2.399	−1.886	−1.541
E_{IL}	(10^{-3} ergs cm^{-1})	−6.830	6.760	−12.400	−2.274	−4.484	6.760
E_{ICL}	(10^{-3} ergs cm^{-1})	1.266	1.717	2.997	1.151	0.788	1.041
E_τ	(10^{-3} ergs cm^{-1})	−8.393	11.215	−26.870	−8.940	−7.395	−8.578
E_f	(10^{-3} ergs cm^{-1})	1.202	1.744	5.012	0.546	1.115	1.161
E_L	(10^{-3} ergs cm^{-1})	0.501	0.501	1.002	0.167	0.344	0.501
E_T	(10^{-3} ergs cm^{-1})	3.597	3.807	4.051	3.530	3.703	3.356

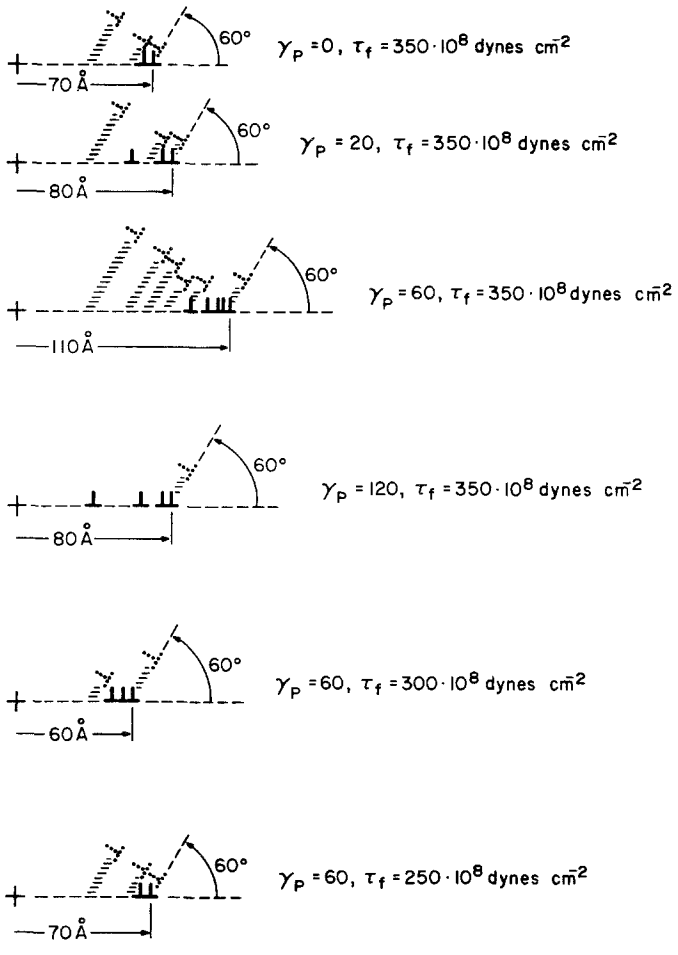

Figure 14 Dislocation configuration of a continuous plastic shear crack in an ordered alloy shown at different values of τ_f and γ_P. Only one quadrant of the configuration is shown since it is symmetrical about the x-and y-axes. The hatched region is the antiphase boundary.

more plastic and hence it reaches the Griffith configuration at bigger size. However, the total energy of the crack is smaller for smaller value of τ_f. The energy contributions associated with the plastic shear crack are shown in Table V for different values of τ_f. It is seen that the crack size at the Griffith configuration is higher for τ_f above and below 300×10^8 dynes cm^{-2}. The contribution to the antiphase boundary energy is also more above and below $\tau_f = 300 \times 10^8$ dynes cm^{-2}, since there are more lattice dislocations generated. The dislocation configuration at the three levels of frictional stress show that the dislocations have moved shorter distances on the slip plane at $\tau_f = 300 \times 10^8$ dynes cm^{-2} and therefore the frictional energy contribution is also small. Therefore, variations in frictional stress τ_f become more important at the high level of applied stress than variations in γ_P. As in the case of a tensile crack, when the applied stress level is small, the component of applied stress on the slip plane will also be small and the crack can be stabilized with smaller friction. When the frictional energy expended is small, the effect of antiphase boundary energy on the crack configuration will be to generate a pair of lattice dislocations on each slip plane bounded by antiphase boundary, thus a configuration similar to that shown in Fig. 1b results.

4. Comparison of the continuous plastic tensile crack with the continuous plastic shear crack

The most favourable slip plane on which the lattice dislocations are generated when a tensile crack expands will be at $\alpha = 60°$ to the crack plane. However, when a slip plane is not available at $\alpha = 60°$ to the crack plane, lattice dislocations are generated on a slip plane which is inclined at an angle nearer to $\alpha = 60°$. It has been found in both disordered and ordered alloys that when the tensile crack expands by generating dislocations

on a slip plane inclined at 60°, the crack requires very high energy to reach the Griffith configuration. As the value of α decreases, the crack tends to become more and more elastic [4]. This is found to be true in ordered alloys also. In the case of a plastic shear crack, the most favourable slip plane is at $\alpha = 0$, i.e. parallel to the crack plane. In ordered alloys, it is found that lattice dislocations are generated in pairs on the slip plane at $\alpha = 0$, therefore they are bounded by antiphase boundary. When the antiphase boundary energy is included in the analysis, it is seen that the shear crack becomes a high energy crack requiring high energy to reach the Griffith configuration. This is also observed in disordered alloys. The effect of antiphase boundary in the behaviour of tensile cracks is to stabilize the crack configuration when the frictional stress alone is not sufficient to do so. The same will be true for the shear crack. When the component of applied stress on the slip plane is small, the frictional stress level can also be small, so that the effect of antiphase boundary energy on the crack configuration is not masked by the frictional energy. The configuration obtained with very small frictional stress values will consist of a pair of lattice dislocations bounded by antiphase boundary on the slip plane. When the frictional stress level is high, the configuration consists of a single lattice dislocation on each slip plane bound to crack by an antiphase boundary. It is felt that frictional stress level in many materials will be small so that crack configurations in ordered alloys should consist of a pair of lattice dislocations on each slip plane bounded by antiphase boundary.

5. Summary and conclusions

A discrete dislocation analysis of the continuous plastic tensile crack and the continuous plastic shear crack in ordered alloys has been carried out in detail in order to determine the behaviour of these two types of cracks. The cracks are assumed to nucleate in a homogeneous medium and expand under constant applied stress, generating lattice dislocations intermittently whenever a reduction in energy can take place. The Griffith configuration is obtained by determining the maximum in the energy versus size curve. It is found that a tensile crack in an ordered alloy can expand, generating lattice dislocations on a slip plane inclined at 90° to the crack plane without a frictional stress. The stability is achieved due to the presence of antiphase boundary energy. A plastic tensile crack which is stabilized by the antiphase boundary energy alone expands due to energy terms which are all reversible and therefore the crack configuration is also reversible.

When the crack expands in the presence of a frictional stress, the frictional energy terms are not reversible and therefore the crack expansion is not a reversible phenomena. It is found that the dislocations are always generated in pairs in the absence of frictional stress. However, in the presence of frictional stress, the generation of lattice dislocations on the slip plane is restricted to a single one on each plane connected to the crack region by the antiphase boundary. While the general characteristics of the energy terms is retained in the total energy of the crack, the effect of including the antiphase boundary energy is reflected in the configurations in a very complex manner due to the fact that the frictional energy term and the antiphase boundary energy term interact. It is found that a variation in frictional stress is more important at higher applied stress levels in determining the dislocation configuration, although the antiphase boundary energy term cannot be neglected. At lower levels of frictional stress, the antiphase boundary energy is more important in determining the configuration of the plastic tensile crack. It is also found that a crack can be stabilized in ordered alloys even when the frictional stress on the slip plane is smaller than the component of the applied stress which moves the dislocation forward on the slip plane. The generation of lattice dislocations on a slip plane parallel to the crack plane ahead of a plastic shear crack is found to always take place in pairs. The distance of separation between the pairs increases with the distance from the tip of the crack. The separation of the pairs is always smaller than the separation between each pair. However, when $\alpha \neq 0$, there is only one dislocation generated on the slip plane and connected to the crack by an antiphase boundary after the first set of lattice dislocations are generated, sometimes in pairs. The continuous plastic shear crack requires very high energy to reach the Griffith configuration when $\alpha = 0$. However, with increasing α the crack tends to be more elastic. The effect of antiphase boundary energy on the shear crack configuration is to stabilize the crack in the same way as it is done for a continuous plastic tensile crack. The effect of frictional stress in the determination of the crack configuration at the Griffith stage is

more important at higher applied stress levels than the antiphase boundary energy, although the antiphase boundary energy cannot be neglected. When the applied stress level is small and the frictional stress is also small, the crack configuration in ordered alloys consists of a pair of lattice dislocations generated on each slip plane and bounded by antiphase boundary. It is expected that this is a more realistic crack configuration in ordered alloys since the frictional stresses are not really large in real materials.

Acknowledgements

The computer time for this project was supported in full through the facilities of the Computer Science Center of the University of Maryland. Financial support for the present study was provided by the US Energy Research and Development Administration under contract No. AT–(40–1)–3935.

References

1. K. JAGANNADHAM and M. J. MARCINKOWSKI, submitted for publication.
2. M. J. MARCINKOWSKI and E. S. P. DAS, *Int. J. Fracture.* **10** (1974) 181.
3. M. J. MARCINKOWSKI and R. W. ARMSTRONG, *J. Appl. Phys.* **43** (1972) 2548.
4. K. SADANANDA, K. JAGANNADHAM and M. J. MARCINKOWSKI, *Phys. Stat. Solid.* **44** (1977) 633.
5. M. J. MARCINKOWSKI, *J. Appl. Phys.* **46** (1975) 496.
6. M. J. MARCINKOWSKI and E. S. P. DAS, *Phys. Stat. Solid.* **A8** (1971) 249.
7. K. JAGANNADHAM and M. J. MARCINKOWSKI, *ibid.* (to be published)
8. M. J. MARCINKOWSKI, "Order–Disorder Transformations in Alloys," edited by H. Warllmont, (Springer–Verlag, New York, 1974) p. 364.
9. SHENG-TI FONG, M. J. MARCINKOWSKI and K. SADANANDA, *Acta Met.* **21** (1973) 799.
10. N. S. STOLOFF and I. L. DILLAMORE, "Ordered Alloys – Structural Applications and Physical Metallurgy," edited by B. H. Kear, C. T. Sims, N. S. Stoloff and J. H. Westbrook, (Clastros, Baton Rouge, 1970).
11. J. P. HIRTH and J. LOTHE, "Theory of Dislocations" (McGraw–Hill, New York, 1968).
12. M. J. MARCINKOWSKI, "Advances in Materials Research," edited by H. Herman (Wiley, New York, 1975) 5382.

Received 10 October and accepted 4 November 1977.